Maria Angela C. Hospenthal and Aimee P. Carswell

Introduction

Radiologic imaging of the structures of the central nervous system (CNS), upper and lower respiratory tract, abdomen, and musculoskeletal system is integral to the diagnosis and management of most human mycoses. Although there are no pathognomonic radiological findings associated with fungal infections, diagnostic imaging combined with clinical data (including historical data of endemic exposures, use invasive devices, coexisting disease or immunodeficiency, surgeries, and duration of illness) can be used to improve diagnostic accuracy and aid in the long-term treatment of certain conditions.

Central Nervous System Imaging

Magnetic resonance imaging (MRI) is superior to computed tomography (CT) in evaluating fungal infections of the brain and has been shown to be more sensitive than CT for detecting abnormalities. CT commonly underestimates the extent of disease in fungal infection [1]. MRI is especially helpful in the early phases of disease when the brain CT may be nondiagnostic. MRI takes advantage of the inherent properties of molecules, especially hydrogen, and manipulates their behavior in an electromagnetic field to generate an image. The composition of tissues and their differences when there is pathology present can therefore be distinguished by altering parameters of the electromagnetic field to see the effect on the molecules of the tissue being evaluated. Terminology to include longitudinal relaxation time (T1) and transverse relaxation time (T2) relates to signal intensities which offer details on specific tissue characteristics. Findings on MRI, such as edema and contrast enhancement are affected by the inflammatory response, which itself is highly dependent on the competence of the immune system. Nevertheless, non-circumscribed, ill-defined areas with little or no contrast enhancement should raise the suspicion for fungal infection [2]. CT of the brain with contrast may be normal initially and thus is more helpful in assessing later stages of infection with eventual findings of focal ring enhancing or hemorrhagic lesions. Other brain imaging modalities include proton magnetic resonance spectroscopy with MRI, which has been reported to be useful in the evaluation of infection due to mucormycosis and cryptococcosis [3]. Diffusion-weighted imaging may also be helpful, particularly in the case of *Aspergillus* infection, as it may help to diagnose early infection or differentiate fungal infection from progressive multifocal leukoencephalopathy and neoplasm [1]. A wide variety of radiologic findings may be found, although intracerebral masses and meningeal enhancement predominate in these infections (Table 6.1).

CNS Mass Lesions

Intracerebral masses are one of the more common findings in fungal brain infections. Predominantly, granulomas or solid-enhancing lesions are reported. In *Aspergillus* infections, these have sometimes been referred to as "aspergillomas." Likewise, in patients with cryptococcal infections, the term "cryptococcoma" has been used. Cryptococcomas can be single or multiple punctate (i.e., miliary) hyperintense round lesions on T2-weighted images (T2WI) usually less than 3 mm in size [4, 5]. Intraparenchymal cryptococcomas show low signal intensity on T1-weighted images (T1WI) and high intensity on T2WI [1, 6, 7]. Granulomas are preferentially seen on the ependyma of the choroid plexus [1]. Immunocompetetent patients are more likely to present with cryptococ-

M. A. C. Hospenthal (✉)
Department of Internal Medicine, Division of Pulmonary/Critical Care Medicine, Audie L. Murphy Veteran Administration Hospital, South Texas Veterans Health Care, 7400 Merton Minter Blvd (111E), San Antonio, TX 78229, USA
e-mail: hospenthal@uthscsa.edu

A. P. Carswell
Department of Diagnostic Radiology, University of Texas Health Science Center at San Antonio, 7703 Floyd Curl Drive, San Antonio, TX 78229, USA

Table 6.1 Abnormalities more commonly seen in central nervous system imaging of fungal infections

Radiological finding	Fungus
Granulomas or solid enhancing lesions	*Aspergillus, Cryptococcus, Histoplasma, Candida, Paracoccidioides*
Abscesses	*Aspergillus, Blastomyces* (epidural), *Coccidioides, Cryptococcus, Candida,* dematiaceous fungi, *Pseudallescheria boydii* (*Scedosporium apiospermum*)
Parenchymal/lepto-meningeal nodules; pseudocysts	*Cryptococcus*
Hemorrhagic/infarcted lesions	*Aspergillus*
Meningeal enhancement	*Blastomyces, Coccidioides* (chronic granulomatous), *Cryptococcus, Histoplasma, Paracoccidioides, Aspergillus*
Hydrocephalus	*Cryptococcus, Coccidioides, Paracoccidioides*

comas [1] and are more likely to demonstrate enhancement in an immunocompetent host, secondary to the ability to mount an immune response [1, 8]. Persistence of cryptococcomas over a prolonged period of time has been documented and found to be inconsistent with active disease [9]. Pseudocysts are also seen in cryptococcal infection, and are CSF-equivalent (low signal intensity on T1WI and high signal intensity on T2WI) that are predominately seen in the basal ganglia, thalami, midbrain, cerebellum, and periventricular matter (Fig. 6.1). Lesions in the basal ganglia and thalami strongly suggest cryptococcal infection [1, 8]. Single- or multiple-enhancing brain lesions have also been reported in *Histoplasma, Candida,* and *Paracoccidioides* infections.

Abscesses are frequently found in fungal brain infections [10]. These lesions can be multiple, hypodense, and may exert little mass effect. They may or may not enhance [11] (Fig. 6.2). Although abscesses occur most commonly in the cerebral hemispheres, they have also been visualized in the cerebellum and brainstem [12]. Organisms reported to cause abscess formation include *Aspergillus, Coccidioides, Cryptococcus,* and *Candida.* Candidal organisms tend to cause focal necrosis producing microabscesses [13, 14]. Less commonly, the dematiaceous moulds and *Pseudallescheria boydii* have been reported to cause one or multiple brain abscesses [15]. CNS abscesses outside the brain parenchyma are not common, although *Blastomyces* has been reported to cause epidural abscesses [16].

Other intracerebral masses associated with fungal pathogens include edematous, hemorrhagic, or infarcted lesions such as those seen in *Aspergillus* infections [11]. The hemorrhagic lesion, usually a consequence of an area of infarction, is an early radiologic sign owing to the angioinvasive nature of certain fungi [10, 17]. A peripheral ring of isointensity or low signal intensity on T2WI relates to a dense population of fungal hyphae containing paramagnetic elements and small areas of hemorrhage [1, 18]. On cross-sectional imaging,
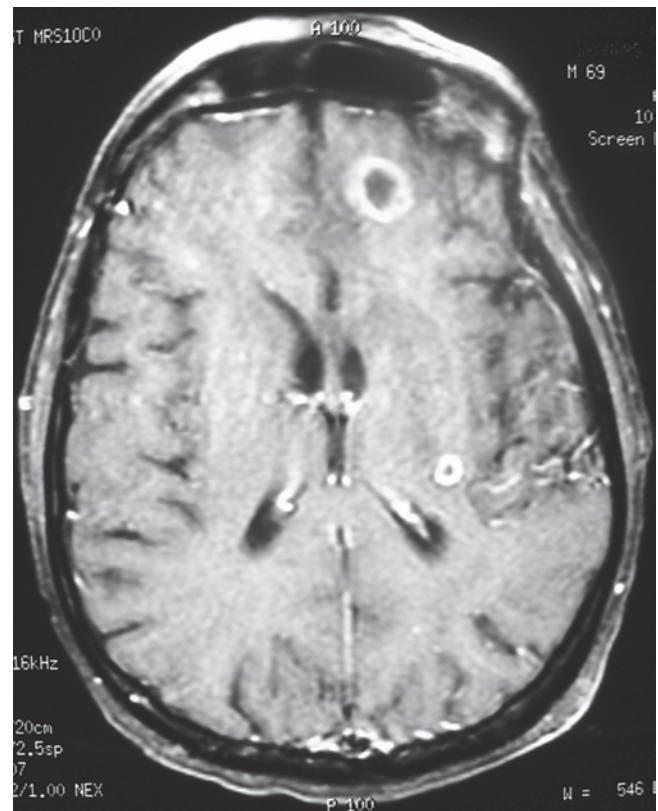
Fig. 6.1 Contrast-enhanced TI transaxial MRI image of the brain demonstrating low-signal-intensity lesions in the bilateral basal ganglia (left greater than right) associated with no significant enhancement, consistent with gelatinous pseudocysts of cryptococcosis. Also note mild meningeal enhancement. *MRI* magnetic resonance imaging
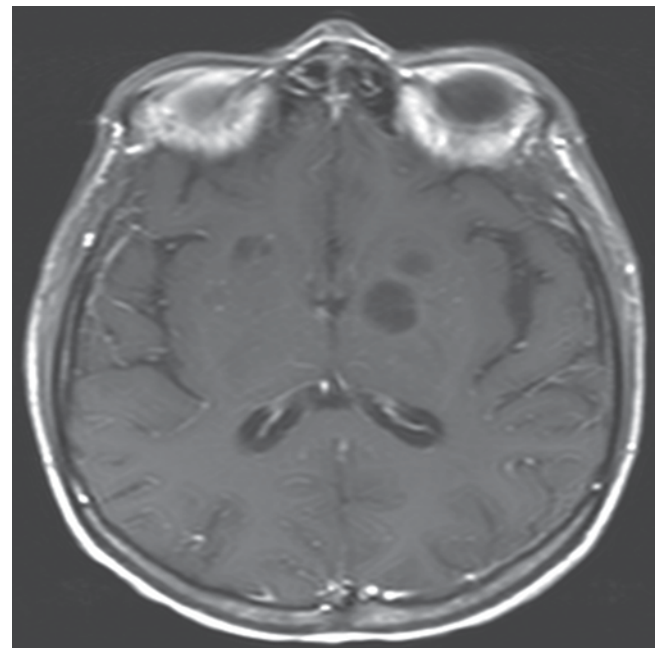
Fig. 6.2 Contrast-enhanced MRI showing multiple ring-enhancing brain abscesses in immunocompromised patient with disseminated aspergillosis. Note the lack of surrounding edema. *MRI* Magnetic resonance imaging. (Courtesy of Dr. D. R. Hospenthal)

these lesions show little or no enhancement or mass effect [11]. Similarly to pyogenic abscesses, fungal abscesses demonstrate decreased diffusion [1, 19].

Meningeal Enhancement

Diffuse enhancement of the meninges on MRI is another common radiological finding of fungal infection of the CNS, thought to be due to active inflammation (meningitis). *Histoplasma, Blastomyces, Coccidioides, Paracoccidioides, Cryptococcus,* as well as *Aspergillus* have all been observed to produce meningeal enhancement. *Coccidioides* meningitis early in its course can cause focal or nodular enhancement in the basal cisterns which represent focal organization of the fungus surrounded by inflammation [20]. Meningeal involvement may be seen secondary to direct extension from fungal infections involving the paranasal sinuses, such as blastomycosis and mucormycosis [1, 21]. Leptomeningeal enhancement in coccidiomycosis has been known to extend into the spinal canal as well [1].

Fig. 6.3 MRI of brain revealing leptomeningeal enhancement and hydrocephalus in a patient with coccidioidomycosis. *MRI* Magnetic resonance imaging

Hydrocephalus

Hydrocephalus is usually a communicating hydrocephalus and is a consequence of meningeal involvement (acutely due to meningeal exudate and later because of meningeal adhesions); it is an additional finding associated with infections by *Cryptococcus, Coccidioides* and *Paracoccidioides* [1, 8, 22] (Fig. 6.3). While CT is helpful in identifying dilated ventricles, MRI appears better in determining the patency of the aqueduct of Sylvius. Other nonspecific CNS radiological findings include early vascular enhancement and diffuse cerebral edema.

Respiratory Tract Imaging

Sinus Imaging

CT is the imaging modality of choice in the evaluation of sinusitis [23]. It is certainly useful in evaluating the extent of fungal sinus disease [24]. The CT scan defines soft tissue invasion, necrosis, early bone erosion and cavernous sinus thrombosis [25]. When findings are suggestive of fungal sinusitis but the diagnosis is uncertain, MRI with or without gadolinium is the best radiological means to further evaluate the disease [23, 24, 26–28]. Central areas of hyperattenuation on CT correspond to hypointense signals on T1WI and signal void with T2WI MRI [29–31]. Early changes in major vessels and intracranial extension are also best seen on MRI, as is possible cavernous sinus thrombosis and embolic phenomena.
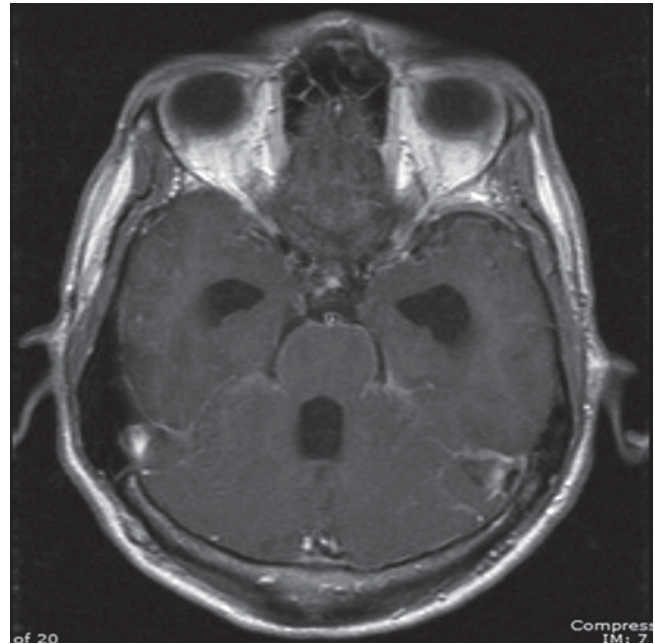
The paranasal sinuses are the most frequently affected, with the maxillary and ethmoid sinuses being the most commonly involved, followed by the sphenoid sinuses. Bilateral involvement is slightly more common than unilateral involvement [32]. Radiologic findings include opacification of multiple paranasal sinuses, with possible demonstration of sinus cavity expansion and erosion of the involved sinus wall. Bone destruction, erosion, and osteomyelitis have been reported in both the invasive and allergic form of *Aspergillus* sinusitis, as well as infections due to Mucorales (agents of mucormycosis) [26, 33, 34] (Fig. 6.4). A soft tissue mass or a sinus "aspergilloma" is reported as a major CT finding of the invasive granulomatous form of fungal sinusitis from *Aspergillus*. It can appear as sinus opacification associated with flocculent calcifications [35] (Fig. 6.5). The mass may either present as a homogenous density or have components of lower attenuation. Intraorbital and/or intracranial extension may occasionally occur [34, 36]. Air–fluid levels may be found though these are rare in either the invasive or noninvasive forms of fungal sinusitis [25]. Other findings include scattered intrasinus high-attenuation areas amid mucosal thickening on unenhanced CT scans.

Pulmonary Imaging

Definitive diagnosis of a pulmonary fungal infection by radiological imaging alone is not possible as other infectious organisms, and likewise, noninfectious pulmonary syndromes,

Fig. 6.4 Transaxial sinus CT of patient with mucormycosis demonstrating osteolysis of the hard palate (*arrow*) and left maxillary sinus mucosal thickening with surrounding soft tissue air. *CT* computed tomography
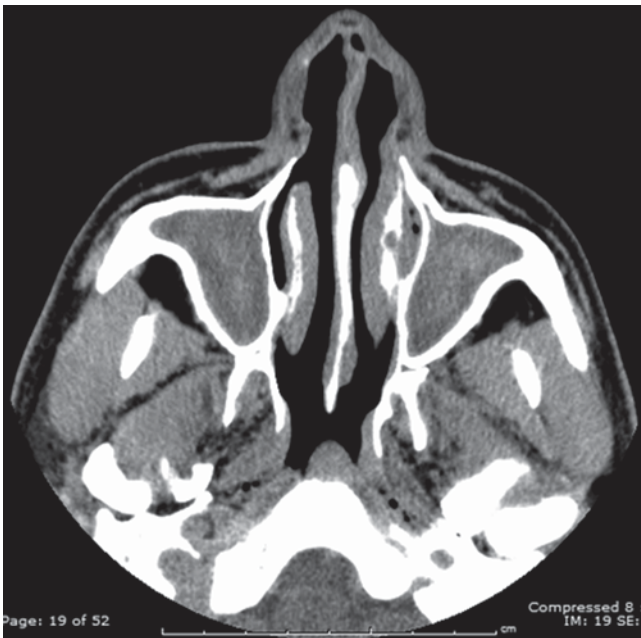
Table 6.2 Abnormalities more commonly seen in pulmonary imaging of fungal infections

Radiological finding	Fungus
Alveolar infiltrates	*Aspergillus*, *Blastomyces*, *Candida*, *Coccidioides*, *Cryptococcus*, *Histoplasma*, *Pneumocystis*, Mucorales
Interstitial infiltrates	*Aspergillus*, *Coccidioides*, *Cryptococcus*, *Histoplasma*, *Paracoccidioides*, *Penicillium*, *Pneumocystis*
Nodules	*Aspergillus*/Mucorales (halo sign), *Candida*, *Coccidioides*, *Cryptococcus*, *Histoplasma*, *Paracoccidioides*, *Pneumocystis*
Masses	*Aspergillus*, *Blastomyces*, *Coccidioides*, *Cryptococcus*, Mucorales
Cavitation	*Aspergillus*/Mucorales (air crescent sign), *Blastomyces*, *Coccidioides*, *Cryptococcus*, *Histoplasma*, *Paracoccidioides*, *Pneumocystis*
Abscesses	*Candida*, *Pseudallescheria* (*Scedosporium*), Mucorales
Adenopathy	*Coccidioides*, *Cryptococcus*, *Histoplasma*
Pleural effusion	*Candida*, *Coccidioides*, *Cryptococcus*, *Histoplasma*, *Pneumocystis*

Fig. 6.5 Transaxial CT image through the sinuses demonstrating high-density opacification of the maxillary sinuses consistent with fungal sinusitis. *CT* computed tomography

can mimic radiological findings [37]. The most useful tools to assess lung infections include chest roentgenography and CT [38–40]. Chest radiography in the earlier stages of fungal disease may be normal, thus CT is the superior imaging modality as it has been shown to reveal abnormalities much earlier than chest X-rays. MRI, though reported to have been useful in the workup for *Pneumocystis* disease, has not been recognized as a significant diagnostic tool for the majority

of pulmonary fungal infections [39]. Fungal infection of the lung presents generally with a wide variety of nonspecific radiographic patterns (Table 6.2).

Airspace and Interstitial Opacities

Nonspecific airspace opacities are the most frequent radiologic findings found with any pulmonary infectious process. Alveolar, "patchy," "air-space," or "mass-like" opacities have been identified in many fungal diseases, often progressing to areas of consolidation in the lung. Alveolar opacities have been noted in both endemic and opportunistic fungal infections. Airspace opacities have been noted as a frequent initial pattern in invasive pulmonary aspergillosis (IPA). Opacities may be unifocal or multifocal and then progress to diffuse consolidation, though segmental areas of consolidation have been noted as one of the most common CT patterns in IPA [41, 42] (Fig. 6.6). Other disease processes resulting from *Aspergillus* infection such as bronchopneumonia, hypersensitivity pneumonitis, chronic necrotizing aspergillosis, and semi-invasive aspergillosis have also presented with alveolar opacities, often progressing to consolidation [38, 41, 43]. Patchy, ill-defined opacities progressing to more diffuse, bilateral airspace consolidation are common findings in blastomycosis (seen with a prevalence of 26–76 %) [21].

Interstitial, "reticular," "reticulonodular," and "linear" opacities have also been observed in many fungal infections. Diffuse bilateral interstitial opacities in a perihilar distribution [37, 44, 45] are the most common pattern seen in *Pneumocystis* infection (Fig. 6.7). Chest CT often reveals perihilar ground-glass opacity in a mosaic pattern with patchy distribution of affected lung interspersed with areas of normal lung, and noted thickening of the interlobular septa [38].
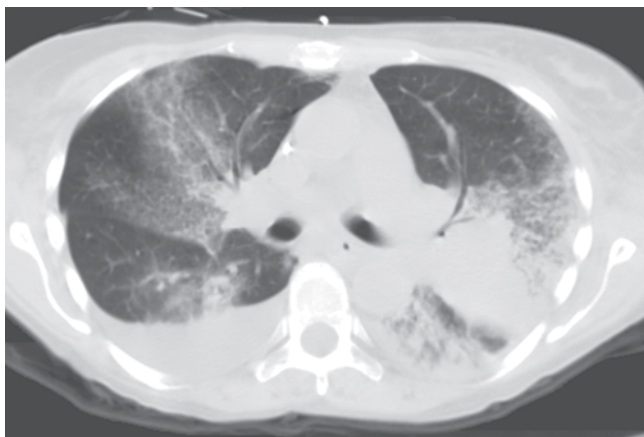
Fig. 6.6 Transaxial CT image through the chest of patient with invasive pulmonary aspergillosis demonstrating diffuse ground-glass opacity and bibasilar consolidation. *CT* computed tomography. (Courtesy of Dr. D. R. Hospenthal)

Fig. 6.7 Chest radiograph showing interstitial prominence and ground-glass opacity in a patient with *Pneumocystis* pneumonia

Interstitial opacities are also the most common pattern seen in cryptococcosis [46]. Ground-glass attenuation may be seen in AIDS patients with this infection. *Aspergillus* is able to affect the lung in a variety of ways, most of which can present in an interstitial pattern. These range from nodular opacities of invasive and semi-invasive disease, mimicking the radiologic findings of reactivation tuberculosis (TB), to coarse reticulation found in chronic hypersensitivity pneumonitis [38, 41]. A miliary or reticulonodular pattern is commonly seen in *Blastomyces* infection. *Coccidioides* pneumonia has been noted with diffuse reticulonodular lesions, especially in the setting of AIDS. Heavy exposure to *Histoplasma* can similarly present with diffuse reticulonodular opacities, such as those found in acute disseminated disease [47]. Other organisms commonly demonstrating interstitial opacities include *Penicillium marneffei* in the setting of HIV infection and paracoccidioidomycosis. In *Paracoccidioides* infection, the "reversed halo sign" of ground-glass opacity surrounded by denser airspace consolidation of crescent and ring shapes, has been reported in 10 % of patients [48, 49]. The lesions predominate in the mid to lower lungs, particularly in the periphery [49]. The reversed halo sign has also be described in zygomycosis and IPA, as well as histoplasmosis and *Pneumocystis jiroveci* pneumonia. In an immunosuppressed patient with reversed halo sign, invasive fungal infection should be considered until proven otherwise [50].

Distribution and location of opacities are also nonspecific. Opacities may be confined to a lobe or they may be diffuse as seen in disseminated disease. Hematogenous candidal spread can manifest as perivascular pulmonary opacities [51]. Allergic bronchopulmonary aspergillosis often presents with fleeting or migratory upper lobe opacities [41]. Phantom opacities which resolve in one segment then reappear in another lung field have also been seen in coccidioidomycosis [51].
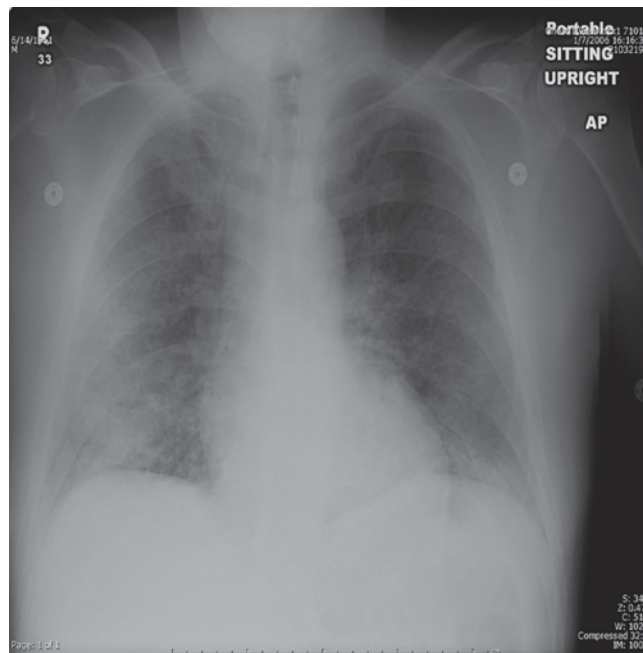
The shape of infiltrates can sometimes aid in the diagnosis. Wedge-shaped opacities, reflecting invasion of blood vessels with subsequent lung infarction, are suggestive of invasive *Aspergillus* or Mucorales [52].

Uncommon pathogens which can cause infections presenting with nonspecific pulmonary opacities include *Fusarium, Trichosporon, Malassezia furfur,* and the phaeohyphomycetes [53].

Nodules

A well-defined nodule, either single or multiple, has been reported as a frequent initial radiographic pattern of IPA [54]. This nodular lesion may be surrounded by a rim of hemorrhage from thrombosis of fungi within pulmonary vessels [55]. Days to weeks after treatment of neutropenia, patients infected with *Aspergillus* may present with ground-glass attenuation around the nodules recognized as the "halo sign" [41, 56, 57] (Fig. 6.8). The "halo sign" is highly suggestive of angioinvasive aspergillosis, but is nonspecific. It is thought that the surrounding ground-glass opacity may be related to hemorrhage from the vascular involvement. Other infectious processes including the mucormycosis, *Candida,* herpes simplex virus, and cytomegalovirus infections, as well as noninfectious processes such as Wegener's granulomatosis, Kaposi's sarcoma, and hemorrhagic metastatic malignancies have also been presented with "halo signs" [58–60]. Nodular lesions may also be observed with branching linear opacities recognized as the "tree-in-bud" pattern seen in *Aspergillus* bronchiolitis [38]. "Tree-in-bud" pattern suggests a small

Fig. 6.8 Transaxial CT image of the chest with a right middle lobe nodule with surrounding ground-glass opacity (halo sign). This is consistent with invasive aspergillosis in an immunocompromised patient. *CT* computed tomography

Fig. 6.9 Transaxial CT image of the chest showing bilateral upper lobe bronchiectasis, right pleural thickening, and right upper lobe ground-glass opacity and aspergilloma (soft tissue mass in preexisting cavity). *CT* computed tomography

airways process; a disease process which may be spread endobronchially. Similar lesions are found in endobronchial spread of mycobacterial, viral, and mycoplasma pneumonia. Nodules from Mucorales can be indistinguishable from IPA. The most common finding in pulmonary cryptococcosis are nodules, solitary or multiple, with or without cavitation, ranging from 5 to 20 mm in size with smooth or irregular margins, associated with other parenchymal findings such as masses and consolidation [61–63]. Miliary nodules are less commonly found in the AIDS patient with cryptococcosis [64]. Other organisms which can present with diffuse nonspecific nodular lesions include disseminated *Candida* and *Histoplasma*. Nodules can turn to "buck shot" calcifications in pulmonary histoplasmosis [52]. Approximately 5 % of those who develop *Coccidioides* pneumonia may develop solitary pulmonary nodules. Infections with *Pneumocystis, Scedosporium,* and *Paracoccidioides* have also demonstrated pulmonary nodules.

Masses

Parenchymal masses may include aspergillomas, 3–5 cm mobile, round or oval masses, usually solitary, and seen in the upper lobe within a preexisting cavity (Fig. 6.9) or ectatic bronchus. These masses may be partially surrounded by a radiolucent crescent (Monod's sign) of varying thickness [41, 65, 66]. This is the pattern most often seen in immunocompetent hosts [66]. Occasionally, coccidioidal infections may leave persistent chest X-ray lesions, most common being the coccidioidoma and the peripheral cavity [51]. The occasional "fungus ball" can form inside the cavity, rupture into the

pleural space and produce an air–fluid level on an upright chest X-ray. Nonspecific mass lesions have been reported in infections with *Cryptococcus, Pneumocystis,* and the Mucorales. As fungal infections may present with nodules and masses which may have irregular or speculated borders, it is not uncommon to mistake them for malignancy. Fungal infections mimicking malignancy include coccidiomycosis, histoplasmosis, aspergillosis, blastomycosis, and cryptococcus. Some have advocated for use of fluorodeoxyglucose (FDG)/positron emission tomography (PET) to differentiate between infection and malignancy; however, there is a high rate of false positives secondary to hypermetabolic nature of fungal infections. However, PET/CT does have a high negative predictive value [67].

Nonparenchymal masses may be seen in the hilar or mediastinal areas. Chronic pulmonary blastomycosis might present with a single large perihilar mass that often warrants a thoracotomy to rule out possible carcinoma. In fact, up to 31 % of patients present with paramediastinal or perihilar masses, which unlike histoplasmosis, rarely contain calcification [21]. Other findings of cryptococcosis in AIDS patients include mediastinal masses.

Cavitation

Virtually any nodular lesion has the potential to cavitate. Nodular lesions seen in *Aspergillus* and Mucorales infections may progress to cavitate to what is recognized as the "air crescent sign" [41, 57, 58, 68]. The air crescent sign represents cavitation of nodules caused by resorption of necrotic tissue by returning neutrophils [55] (Fig. 6.10). It is usually unilateral and frequently in the upper lobes [38]. Other nodules, single or multiple, can cavitate and then proceed to either diffuse pulmonary consolidation or abrupt development of large wedge-shaped pleural-based lesions mimicking bland
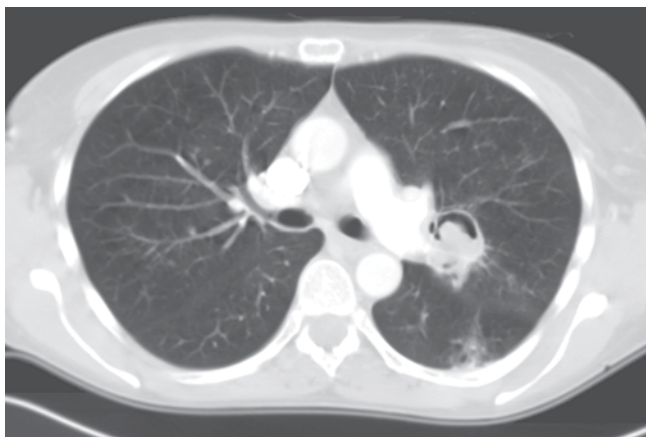
Fig. 6.10 Transaxial CT scan of the chest demonstrates a cavity in the left upper lobe with dependent soft tissue in a patient with invasive aspergillosis (air crescent sign). *CT* computed tomography. (Courtesy of Dr. D. R. Hospenthal)

infarction. Thin- or thick-walled cavities as well as cavitary infiltrates can appear in subacute invasive aspergillosis and chronic progressive coccidioidomycosis, both of which can mimic TB [52]. Approximately 5% of those who develop *Coccidioides* pneumonia develop thin-walled solitary cavities, typically near the pleura (Fig. 6.11). A chronic form of *Coccidioides* pneumonia presents as a slowly progressive fibrocavitary process of biapical fibronodular lesions with retraction and cavitation. In pulmonary histoplasmosis, upper lobe cavities are common, except in those with HIV infection. Cavitary infiltrates have also been demonstrated in disseminated disease. Fibrotic apical infiltrates with cavitation have been reported in chronic pulmonary histoplasmosis which can be confused with TB infection or co-infection on chest X-ray [52]. Other fungal infections reported to cause cavitary disease include sporotrichosis and paracoccidioidomycosis; nodular areas are sometimes confluent, often in the lower lobes; cavitation occurs in one third of cases. Cavitation from blastomycosis is unusual and not as commonly seen as in mycobacterial or *Histoplasma* infections. Cryptococcal infection may present with cavitary masses or nodules, though this is uncommonly seen in the setting of AIDS infection. In cancer patients infected with *Pneumocystis* previously given prophylactic aerosolized pentamidine, upper lobe infiltrative disease suggestive of tuberculosis may be seen, but cavitary lesions are very uncommon.

Adenopathy

Adenopathy has been observed commonly in histoplasmosis, coccidioidomycosis, and cryptococcosis. In acute histoplasmosis, a common finding in a low-level exposure includes enlarged hilar or mediastinal lymphadenopathy. In heavy exposure, the mediastinal adenopathy is usually accompanied by diffuse reticulonodular infiltrates as mentioned previ-

ously. There is potential extensive calcification of paratracheal, hilar, and subcarinal lymph nodes [69]. Occasionally, these lymph nodes combine to form granulomas which can rupture and cause chronic inflammation with subsequent diffuse mediastinal fibrosis [70], or more commonly—a localized mediastinal mass [71]. This process, known as fibrosing mediastinitis, can partially obstruct airways, vessels, and the esophagus [71]. Mediastinal lymphadenopathy is uncommon in disseminated histoplasmosis, occurring at less than 10% in one series. Coccidioidomycosis is also noted to present with bilateral hilar adenopathy. Prominent hilar adenopathy is occasionally seen in cryptococcosis. Radiologic findings vary widely in *Pneumocystis* infections but lymphadenopathy is extremely rare.

Pleural Abnormalities

The effect of fungal infections on the pleura and pleural cavity is not as common as the other previously described radiologic findings. Ultrasonography is useful in the initial detection and subsequent management of pleural effusions but the main imaging modality to visualize the pleura is CT; cross-sectional CT imaging, in particular, can be used to aid in the diagnosis and assessment of severity of disease as well guide interventional diagnostic procedures [72]. Pleural thickening with concomitant upper lobe consolidation potentially progressing to cavitation over weeks to months can be seen in semi-invasive pulmonary aspergillosis [41]. Pleural effusions have been noted in candidal pneumonia. Large parapneumonic effusions have been documented in coccidioidomycosis. Other organisms that have demonstrated pleural effusions include *Cryptococcus, Histoplasma,* and *Scedosporium.* Effusions are unusual in *Blastomyces* and *Pneumocystis* infections.

Airway Abnormalities

Tracheal or bronchial wall mucosal thickening along with airway plaques can be seen in invasive aspergillosis [38, 41]. *Cryptococcus* infection of the larynx can present on CT soft tissue images of the neck as vocal cord irregularities and asymmetric enlargement [73]. Cylindric bronchiectasis in a central distribution, as well as traction bronchiectasis, has also been noted on CT images of various forms of *Aspergillus* as well as *Paracoccidioides* infections [41, 74]. An endobronchial lesion from *Pennicillium marneffei* presented as pulmonary infiltrates due to the resultant postobstructive pneumonia [75].

Miscellaneous

Hematogenous spread of *Candida* can cause multiple abscesses in the body, including the lungs [76]. Mucormycosis and pseudallescheriasis have also been reported to cause pulmonary abscesses [77, 78]. Atelectasis, which may ap-

Fig. 6.11 Transaxial CT scan through the chest and chest radiograph demonstrating a thin-walled cavity in the left upper lobe in an asymptomatic patient proven to have coccidioidomycosis. *CT* computed tomography. (Courtesy of Dr. D. R. Hospenthal)
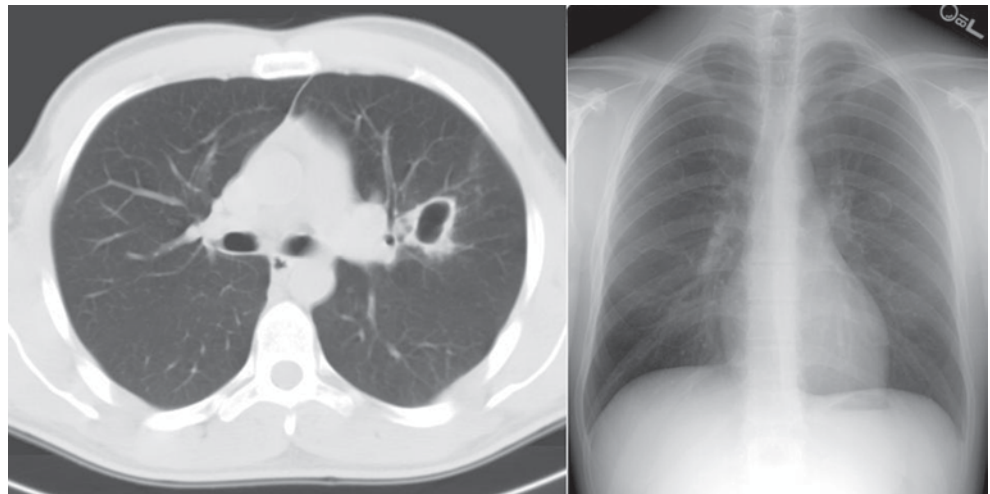
pear as bilateral lower lobe consolidation, has been noted in various pathologic processes caused by *Aspergillus* [41]. Thin-walled cysts or pneumatoceles can form in *Pneumocystis* infections, especially in those patients receiving prophylaxis with aerosolized pentamidine and TMP/SMX [44]. These upper lobe lesions increase the risk of developing pneumothoraces. End-stage honeycombing can be seen in the chronic form of hypersensitivity pneumonitis secondary to *Aspergillus* [41]. Pseudoaneurysm of the aortic arch has been noted in IPA [79].

Multidetector CT (MDCT) angiography takes advantage of the angioinvasive nature of *Aspergillus* and allows direct detection of vessel occlusion up to a peripheral lesion with high-resolution images demonstrating possibly the earliest sign of disease from *Aspergillus* [80].

Fig. 6.12 Constrast-enhanced CT scan through the abdomen showing multiple subcentimeter low-attenuation hepatic and splenic lesions in patient with chronic disseminated candidiasis. *CT* computed tomography. (Courtesy of Dr. D. R. Hospenthal)

Abdominal Imaging

CT or MRI should be the initial imaging modality used to evaluate the abdomen for signs of fungal infection. Ultrasonography, a safer, low-cost method, may then be obtained to follow up noted disease processes. Serial ultrasounds every 3–4 weeks may be used to monitor response to therapy, typically observed as decreasing size and number of lesions or may be useful in detecting evolution of new lesions [81]. Once the ultrasound is clear, a repeat CT or MRI is suggested. Similar to other affected organs mentioned above, radiologic findings of abdominal fungal infections are varied to include nonspecific lesions, organomegaly, and lymphadenopathy.

Target Lesions

Candida is one of the main fungi to cause abdominal disease. In patients with dysphagia or odynophagia, fulminant *Can-*

dida esophagitis can present as longitudinal plaques along the esophagus. Large filling defects from aggregated plaques can appear as "cobblestoning" in severe disease [82, 83]. Involvement of the liver, biliary tree, pancreas, and spleen has been documented in disseminated disease [84]. Target lesions seen in the spleen and liver resulting from candidal infection are most commonly detected on CT or MRI after the resolution of neutropenic episodes [81] (Fig. 6.12). On abdominal CT, chronic disseminated (formerly hepatosplenic) candidiasis is characterized by small, round, low-attenuation lesions scattered through the liver and spleen with occasional peripheral enhancement [85]. Occasionally, multiple small low-attenuation lesions in the spleen and kidneys are seen without lymph node enlargement or hepatosplenomegaly [86]. Four dominant findings on ultrasound have been described. Most commonly, uniform hypoechoic lesions are

noted and can be seen in conjunction with the other three patterns. A "wheel within a wheel" pattern can be seen representing an outer hypoechoic area of fibrosis surrounding a hyperechoic area of inflammation. A "bull's eye" measuring from 1 to 4 cm may evolve from primary lesions. "Echogenic foci," usually seen late, correlate with central fibrosis, calcifications, or both [87]. MRI has been reported to be superior to CT in characterizing chronic disseminated candidiasis. Although relatively rare, disseminated *Coccidioides* infections have been reported to affect the spleen; detected as target lesions with central areas of low attenuation on CT imaging [86, 88].

Organomegaly

Moderate to marked enlargement of the liver, spleen, and adrenals have been noted in disseminated histoplasmosis [86, 89, 90]. Cryptococcal infections have also been reported to produce marked splenomegaly and mild hepatomegaly [86, 91].

Lymphadenopathy

Enlarged lymph nodes with or without central or diffuse low attenuation are seen in the majority of patients with abdominal histoplasmosis [86, 91–93]. Cryptococcal infection has also been noted to have enlarged lymph nodes on CT imaging.

Miscellaneous

Abdominal abscesses have been reported in deeply invasive candidiasis [84, 94]. Uncommon findings in disseminated histoplasmosis include colonic wall thickening, and omental and mesenteric infiltration [86]. Adrenal masses, vascular occlusion, and extensive necrosis have also been noted. Multiple scattered low-attenuation foci can persist from focal scarring and granulomatous change which may eventually result in calcifications.

Musculoskeletal Imaging

MRI and nuclear imaging modalities are the most sensitive and specific methods for the detection of fungal infections in the skeletal system (Fig. 6.13) [95]. Osteomyelitis is the most frequent radiologic finding associated with skeletal fungal infections, though radiographic appearance is nonspecific and indistinguishable among fungi or from bacterial or neoplastic disease. Bone MRI may be sensitive for picking

Fig. 6.13 Bone scan demonstrates increased uptake at approximately T8, T11, and T12. Although this patient had coccidioidomycosis, these findings are nonspecific and could represent another infection, inflammatory or neoplastic process.
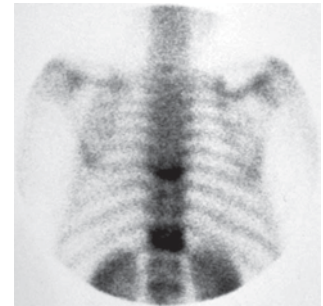
up early lesions of osteomyelitis and is typically useful in assessing infections of the feet and vertebral column [96, 97]. Technetium uptake is dependent on blood flow, while gallium uptake is dependent on the presence of leukocytes in the area of inflammation [98]. Though positive bone scans may be seen as early as 24 h following the onset of infection, a normal scan may be the result of scanning prior to the onset of reactive hyperperfusion.

Osteomyelitis

In blastomycosis, the vertebral column, ribs, skull, and the epiphyseal ends of long bones are most commonly affected [99, 100]. In the tubular bones of the extremities, eccentric saucer-shaped erosions may be seen beneath a cutaneous abscess. Epiphyseal or metaphyseal focal or diffuse osteomyelitis has been reported as well as cystic foci or diffuse "moth-eaten" areas in the carpal or tarsal areas [101]. Histoplasmosis similarly affects the pelvis, skull, ribs, and small tubular bones.

Radiologically, osteoporosis, joint-space narrowing, and bony erosion may be seen similar to tuberculosis. *Candida* osteomyelitis usually occurs in the setting of disseminated candidiasis. The axial spine of adults and the long bones of children are primarily affected [101]. The most common abnormalities include bone destruction, soft tissue extension/swelling, intervertebral space/joint space narrowing, and epidural abscesses. Hypointense MRI images on T1WI as well as hyperintense images on T2WI were noted [102]. Irregularities of subchondral bone have also been noted [103]. Coccidioidomycosis also primarily affects the vertebral column and ribs. There is a tendency to involve multiple segments of the vertebrae, sometimes with "skip lesions" [99]. Radiographs reveal periostitis as well as multiple well-demarcated lytic foci in the metaphyses of long tubular bones and in bony prominences (Fig. 6.14). In the spine, one or more vertebral bodies may be involved, typically with paraspinal masses and contiguous rib lesions [103]. Cryptococcosis presents with nonspecific radiographic features to include osteolytic lesions with discrete margins, mild or absent

Fig. 6.14 Plain radiograph of the right ankle showing a lytic lesion in the medial aspect of the distal tibia secondary to coccidioidomycosis

surrounding sclerosis, and little or no periosteal reaction [104]. Mucormycosis generally causes osteolytic changes to the skull or face [103]; periosteal thickening and bony disruption have been noted on CT scan [105]. With Madura foot (eumycotic mycetoma), a chronic granulomatous disease of the subcutaneous tissues and bone, standard X-rays may reveal abnormalities, though CT has been reported to be more sensitive in the earlier stages of the disease. Typically, single or multiple bony defects with extensive soft tissue and bony disruption occurring with sclerosis and periostitis are seen [103]. Other organisms reported to cause radiologic abnormalities of soft tissue and bone include *Scedosporium, Paecilomyces, Pseudallescheria boydii,* and *Sporothrix schenckii* [15, 78, 103, 106, 107]. Osseous and disk-space destruction and a paraspinal mass, resembling those of TB have been reported in aspergillosis [103].

References

1. Jain KK, Mittal SK, Kumar S, Gupta RK. Imaging features of central nervous system fungal infections. Neurol India. 2007;55:241–50.
2. Aribandi M, Bazan C, Rinaldi MG. Magnetic resonance imaging findings in fatal primary cerebral infection due to *Chaetomium strumarium*. Australas Radiol. 2005;49:166–9.
3. Siegal JA, Cacayorinb ED, Nassif AS, et al. Cerebral mucormycosis: proton MR spectroscopy and MR imaging. Magn Reson Imaging. 2000;18:915–20.
4. Miszkiel KA, Hall-Craggs MA, Miller RF, et al. The spectrum of MRI findings in CNS cryptococcosis in AIDS. Clin Radiol. 1996;51:842–50.
5. Tan CT, Kuan BB. Cryptococcus meningitis, clinical–CT scan considerations. Neuroradiology. 1987;29:43–6.
6. Ho TL, Lee H-J, Lee K-W, Chen W-L. Diffusion-weighted and conventional magnetic resonance imaging in cerebral cryptococcoma. Acta Radiol. 2005;46:411–4.
7. Kamezawa T, Shimozuru T, Niiro M, Nagata S, Kuratsu J. MRI of a cerebral cryptococcal granuloma. Neuroradiology. 2000;42:441–3.
8. Saigal GS, Post JD, Lolayckar S, Murtaza A. Unusual presentation of central nervous system cryptococcal infection in an immunocompetent patient. Am J Neuroradiol. 2005;26:2522–6.
9. Hospenthal DR, Bennett JE. Persistence of cryptococcomas on neuroimaging. Clin Infect Dis. 2000;31:1303–6.
10. DeLone DR, Goldstein RA, Petermann G, et al. Disseminated aspergillosis involving the brain: distribution and imaging characteristics. AJNR Am J Neuroradiol. 1999;20:1597–604.
11. Okafuji T, Yabuuchi H, Nagatoshi Y, Hattanda Y, Fukuya T. CT and MR findings of brain aspergillosis. Comput Med Imaging Graph. 2003;27:489–92.
12. Banuelos AF, Williams PL, Johnson RH, et al. Central nervous system abscesses due to *Coccidioides* species. Clin Infect Dis. 1996;22:240–50.
13. Chaabane M, Krifa H, Ladeb MF, et al. Cerebral candidiasis: CT appearance. Pediatr Radiol. 1989;19:436.
14. Lai PH, Lin SM, Pan HB, Yang CF. Disseminated miliary cerebral candidiasis. Am J Neuroradiol. 1997;18:1303–6.
15. Fleming RV, Walsh TJ, Anaissie EJ. Emerging and less common fungal pathogens. Infect Dis Clin North Am. 2002;16:915–33.
16. Roos KL, Bryan JP, Maggio WW, Jane JA, Scheld WM. Intracranial blastomycosis. Medicine (Baltimore). 1979;66:224–35.
17. Yamada Y, Shrier DA, Rubio A, et al. Imaging findings in intracranial aspergillosis. Acad Radiol. 2002;9:163–71.
18. Cox J, Murtagh FR, Wilfong A, Brenner J. Cerebral aspergillosis: MR imaging and histopathologic correlation. Am J Neuroradiol. 1992;13:1489–92.
19. Gaviani P, Schwartz RB, Hedley-Whyte T, Ligon KL, et al. Diffusion-weighted imaging of cerebral infection. Am J Neuroradiol. 2005;26:1115–21.
20. Erly WK, Bellon RJ, Seeger JF, Carmody RFMR. Imaging of acute coccidioidal meningitis. Am J Neuroradiol. 1999;20:509–14.
21. Fang W, Washington L, Kumar N. Imaging manifestations of blastomycosis: a pulmonary infection with potential dissemination. Radiographics. 2007;27:641–55.
22. Gasparetto EL, Liu CB, de Carvalho NA, Rogacheski E. Central nervous system paracoccidioidomycosis: imaging findings in 17 Cases. J Comput Assist Tomogr. 2003;27:12–7.
23. Cornelius RS, Maritn J, Wippold FJ, et al. ACR appropriateness criteria sinonasal disease. J Am Col Rad. 2013;10:241–6.
24. Leo G, Triulszi F, Incorvaia C. Sinus imaging for diagnosis of chronic rhinosinusitis in children. Curr Allergy Asthma Rep. 2012;12:136–43.

25. Blitzer A, Lawson W. Fungal infections of the nose and paranasal sinuses: part I. Otolaryngol Clin North Am. 1993;26:1007–35.
26. Manning SC, Merkel M, Kriesel K, Vuitch F, Marple B. Computed tomography and magnetic resonance diagnosis of allergic fungal sinusitis. Laryngoscope. 1997;107:170–6.
27. Groppo ER, El-Sayed IH, Aiken AH, et al. Computed tomography and magnetic resonance imaging characteristics of acute invasive fungal sinusitis. Arch Otolaryngol Head Neck Surg. 2011;137:1005–10.
28. Fawaz SA, Ezzat WF, Salman MI. Sensitivity and specificity of computed tomography and magnetic resonance imaging in the diagnosis of isolated sphenoid sinus diseases. Laryngoscope. 2011;121:1584–9.
29. Reddy CE, Gupta AK, Singh P, et al. Imaging of granulomatous and chronic invasive fungal sinusitis: comparison with allergic fungal sinusitis. Otolaryngol Head Neck Surg. 2010;143:294–300.
30. Ilica AT, Mossa-Basha M, Maluf F, et al. Clinical and radiologic features of fungal diseases of the paranasal sinuses. J comput Assist Tomogr. 2012;36:570–6.
31. Seo YJ, Kim J, Kim K, et al. Radiologic characteristics of sinonasal fungus ball: an analysis of 119 cases. Acta Radiol. 2011;52:790–5.
32. Dahniya MH, Makkar R, Grexa E, et al. Appearances of paranasal fungal sinusitis on computed tomography. Br J Radiol. 1998;71:340–4.
33. Terk MR, Underwood DJ, Zee CS, Colletti PM. MR imaging in rhinocerebral and intracranial mucormycosis with CT and pathological correlation. Magn Reson Imaging. 1992;10:81–7.
34. Jung JH, Cho GS, Chung YS. Clinical characteristics and outcome in patients with isolated sphenoid sinus aspergilloma. Auris Nasus Larynx. 2013;40:189–93.
35. Yoon JH, Na DG, Byun HS, Koh YH, Chung SK, Dong HJ. Calcification in chronic maxillary sinusitis: comparison of CT findings with histopathologic results. Am J Neuroradiol. 1999;20:571–4.
36. Chandrasekharan R, Thomas M, Rupa V. Comparative study of orbital involvement in invasive and non-invasive fungal sinusitis. J Laryngol Otol. 20112;126:152–8.
37. Boiselle PM, Tocino I, Hooley RJ, et al. Chest radiograph interpretation of *Pneumocystis carinii* pneumonia, bacterial pneumonia, and pulmonary tuberculosis in HIV-positive patients: accuracy, distinguishing features, and mimics. J Thorac Imaging. 1997;12:47–53.
38. Franquet T, Gimenez A, Hidalgo A. Imaging of opportunistic fungal infections in the immunocompromised patient. Eur J Radiol. 2004;51:130–8.
39. Reynolds JH, Banerjee AK. Imaging pneumonia in immunocompetent and immunocompromised individuals. Curr Opin Pulm Med. 2012;18:194–201.
40. Marom EM, Kontoyiannis DP. Imaging studies for diagnosis invasive fungal pneumonia in immunocompromised patients. Curr Opin Infect Dis. 2011;24:309–14.
41. Gotway MB, Dawn SK, Caoili EM, Reddy GP, Araoz PA, Webb WR. The radiologic spectrum of pulmonary *Aspergillus* infections. J Comput Assist Tomogr. 2002;26:159–73.
42. Kami M, Kishi Y, Hamaki T, et al. The value of the chest computed tomography halo sign in the diagnosis of invasive pulmonary aspergillosis: an autopsy-based retrospective study of 48 patients. Mycoses. 2002;45:287–94.
43. Kim SY, Lee KS, Han J, et al. Semiinvasive pulmonary aspergillosis: CT and pathologic findings in six patients. AJR Am J Roentgenol. 2000;174:795–8.
44. Goodman PC. Pneumocystis carinii pneumonia. J Thorac Imaging. 1991;6:16–21.
45. Primack SL, Muller NL. High-resolution computed tomography in acute diffuse lung disease in the immunocompromised patients. Radiol Clin North Am. 1994;32:731–44.
46. Feigin DS. Pulmonary cryptococcosis: radiologic-pathologic correlates of its three forms. AJR Am J Roentgenol. 1983;141:1263–72.
47. Conces DJ, Stockberger SM, Tarver RD, Wheat LJ. Disseminated histoplasmosis in AIDS: findings on chest radiographs. AJR Am J Roentgenol. 1993;160:15–9.
48. Gasparetto EL, Escuissato DL, Davaus T, et al. Reversed halo sign in pulmonary paracoccidioidomycosis. AJR Am J Roentgenol. 2005;184:1932–4.
49. Barreto MM, Marchiori E, Amorim VB, Zanetti G, et al. Thoracic paracoccidiomycosis: radiographic and CT findings. Radiographics. 2012;32:71–84.
50. Marchiori E, Zanetti G, Hochhegger B, Irion KL, et al. Reversed halo sign on computed tomography: state-of-the-art review. Lung. 2012;190:389–94.
51. Bayer AS. Fungal pneumonias: pulmonary coccidioidal syndromes (part I). Chest 1981;79:575–83.
52. Davies SF. An overview of pulmonary fungal infections. Clin Chest Med. 1987;8:495–512.
53. Walsh TJ, Hiemenz JW, Anaissie E. Recent progress and current problems in treatment of invasive fungal infections in neutropenic patients. Infect Dis Clin North Am. 1996;10:365–400.
54. Orr DP, Myerowitz RL, Dubois PJ. Patho-radiologic correlation of invasive pulmonary aspergillosis in the immunocompromised host. Cancer. 1978;41:2028–39.
55. Tanaka N, Matsumoto T, Miura G, Emoto T, Matsunaga N. HRCT findings of chest complications in patients with leukemia. Eur Radiol. 2002;12:1512–22.
56. Kim Y, Lee KS, Jung KJ, Han J, Kim JS, Suh JS. Halo sign on high resolution CT: findings in spectrum of pulmonary diseases with pathologic correlation. J Comput Assist Tomogr. 1999;23:622–6.
57. Kuhlman JE, Fishman EK, Siegelman SS. Invasive pulmonary aspergillosis in acute leukemia: characteristic findings on CT, the CT halo sign, and the role of CT in early diagnosis. Radiology. 1985;157:611–4.
58. McAdams HP, Rosado de Christenson M, Strollo DC, Patz EF. Pulmonary mucormycosis: radiologic findings in 32 cases. AJR Am J Roentgenol. 1997;168:1541–8.
59. Primack SL, Hartman TE, Lee KS, Muller NL. Pulmonary nodules and the CT halo sign. Radiology. 1994;190:513–5.
60. Chung JH, Godwin JD, Chien JW, Pipavath SJ. Case 160: pulmonary mucormycosis. Radiology. 2010;256:667–70.
61. Khoury MB, Godwin JD, Ravin CE, Gallis HA, Halvorsen RA, Putman CE. Thoracic cryptococcosis: immunologic competence and radiologic appearance. AJR Am J Roentgenol. 1984;141:893–6.
62. Zinck SE, Leung AN, Frost M, Berry GJ, Muller NL. Pulmonary cryptococcosis: CT and pathologic findings. J Comput Assist Tomogr. 2002;26:330–4.
63. Zlupko GM, Fochler FJ, Goldschmidt ZH. Pulmonary cryptococcosis presenting with multiple pulmonary nodules. Chest. 1980;77:575.
64. Cameron ML, Barlett JA, Gallis HA, Waskin HA. Manifestations of pulmonary cryptococcosis in patients with acquired immunodeficiency syndrome. Rev Infect Dis. 1991;13:64–7.
65. Irwin A. Radiology of the aspergilloma. Clin Radiol. 1966;18:432–8.
66. Yoon SH, Park CM, Goo JM, Lee HJ. Pulmonary aspergillosis in immunocompetent patients without air-meniscus sign and underlying lung disease: CT findings and histopathologic features. Acta Radiol. 2011;52:756–61.
67. Guimarães MD, Marchiori E, de Souza Portes Meirelles G, Hochhegger B, et al. Fungal infection mimicking pulmonary malignancy: clinical and radiological characteristics. Lung. 2013;191:655–62.
68. Lee FY, Mossad SB, Adal KA. Pulmonary mucormycosis: the last 30 years. Arch Intern Med. 1999;159:1301–9.
69. Koksal D, Bayiz H, Mutluay N, et al. Fibrosing mediastinitis mimicking bronchogenic carcinoma. J Thorac Dis. 2013;5:E5–E7.
70. Sherrick AD, Brown LR, Harms GF, Myers JL. The radiographic findings of fibrosing mediastinitis. Chest. 1994;106:484–9.

71. Devaraj A, Griffin N, Nicholson AG, et al. Computed tomography findings in fibrosing mediastinitis. Clin Radiol. 2007;62:781–6.

72. Helm EJ, Matin TN, Gleeson FV. Imaging of the pleura. J Magn Reson Imaging. 2010;32:1275–86.

73. McGregor DK, Citron D, Shahab I. Cryptococcal infection of the larynx simulating laryngeal carcinoma. South Med J. 2003;96:74–7.

74. Funari M, Kavakama J, Shikanai-Yasuda MA, et al. Chronic pulmonary paracoccidioidomycosis (South American blastomycosis): high resolution CT findings in 41 patients. AJR Am J Roentgenol. 1999;173:59–64.

75. Joosten SA, Hannan L, Heroit G, et al. Penicillium marneffei presenting as an obstructing endobronchial lesion in an immunocompetent host. Eur Respir J. 2012;39:1540–3.

76. Masur H, Rosen PP, Armstrong D. Pulmonary disease caused by *Candida* species. Am J Med. 1977;63:914–25.

77. Rinaldi MG. Zygomycosis. Infect Dis Clin North Am. 1989; 3:19–41.

78. Travis LB, Roberts GD, Wilson WR. Clinical significance of *Pseudallescheria boydii*: a review of 10 years' experience. Mayo Clin Proc. 1985;60:531–7.

79. Koral K, Hall TR. Mycotic pseudoaneurysm of the aortic arch: an unusual complication of invasive pulmonary aspergillosis. Clin Imaging. 2000;24:279–82.

80. Sonnet S, Buitrago-Tellez CH, Tamm M, Christen S, Steinbrich W. Direct detection of angioinvasive pulmonary aspergillosis in immunosuppressed patients: preliminary results with high-resolution 16-MDCT angiography. Am J Roentgenol. 2005;184:746–51.

81. Karthaus M, Huebner G, Elser C, Geissler RG, Heil G, Ganser A. Early detection of chronic disseminated *Candida* infection in leukemia patients with febrile neutropenia: value of computer-assisted serial ultrasound documentation. Ann Hematol. 1998;77:41–5.

82. Sinha R, Rajesh A, Rawat S, et al. Infections and infestations of the gastrointestinal tract. Part 1: bacterial, viral, and fungal infections. Clin Radiol. 2012;67:484–94.

83. Levine MS, Rubesin SE. Diseases of the oesophagus: diagnosis with esophagography. Radiology. 2005;237:414–27.

84. Ostrosky-Zeichner L, Rex JH, Bennett J, Kullberg BJ. Deeply invasive candidiasis. Infect Dis Clin North Am. 2002;16:821–35.

85. Kontoyiannis DP, Luna MA, Samuels BI, Bodey GP. Hepatosplenic candidiasis: a manifestation of chronic disseminated candidiasis in infections of the liver. Infect Dis Clin North Am. 2000;14:721–39.

86. Radin R. HIV infection: analysis in 259 consecutive patients with abnormal abdominal CT findings. Radiol. 1995;197:712–22.

87. Pastakia B, Shawker TH, Thaler M, O'Leary T, Pizzo PA. Hepatosplenic candidiasis: wheels within wheels. Radiology 1988;166:417–21.

88. Anstead GM, Graybill JR. Coccidioidomycosis. Infect Dis Clin N Am. 2006;20:621–43.

89. Radin DR. Disseminated histoplasmosis: abdominal CT findings in 16 patients. AJR Am J Roentgenol. 1991;157:955–8.

90. Grover SB, Midha N, Gupta M, et al. Imaging spectrum in disseminated histoplasmosis: case report and brief review. Australas Radiol. 2005;49:175–8.

91. Coskun ZU, Mathews D, Weatherall P, et al. Cryptococcal lymphadenitis and massive splenomegaly in an immunocompromised patient. Clin Nucl Med. 2007;32:314–6.

92. Heller HM, Wu CC, Pierce VM, et al. A 29 year old man with abdominal pain, fever, and weight loss. N Engl J Med. 2013;369:1453–61.

93. Mardi K, Kaushal V. Cryptococcal mesenteric lymphadenitis in an immunocompromised host. Inidan J Sex Transm Dis. 2012;33:60–1.

94. Sanavi RS, Afshar R, Gashti HN. Fungal abdominal wall abscess in a renal transplant recipient. Saudi J Kidney Dis Transpl. 2006;17:383–5.

95. Pineda C, Vargas A, Rodriguez AV. Imaging of osteomyelitis: current concepts. Infect Dis Clin North Am. 2006;20:789–825.

96. Kapoor A, Page S, Lavalley M, et al. Magnetic resonance imaging for diagnosing foot osteomyelitis: a meta-analysis. Arch Intern Med. 2007;167:125.

97. Karchevsky M, Schweitzer ME, Morrison WB, et al. MRI findings of septic arthritis and associated osteomyelitis in adults. Am J Roentgenol. 2004;182:119.

98. Bonakdar-pour A, Gaines VD. The radiology of osteomyelitis. Orthop Clin North Am. 1983;14:21–37.

99. Sapico FL, Montogmerie JZ. Vertebral osteomyelitis. Infect Dis Clin North Am. 1990;4:539–50.

100. Saccente M, Woods GL. Clinical and laboratory update on blastomycosis. Clin Microbiol Rev. 2010;23:367–81.

101. Katzenstein D. Isolated *Candida* arthritis. Report of a case and definition of a distinct clinical syndrome. Arthritis Rheum. 1985;28:1421–4.

102. Gamaletsou MN, Kontoyiannis DP, Sipsas NV, et al. Candida osteomyelitis: analysis of 207 pediatric and adult cases (1970–2011). Clin Infect Dis. 2012;55:1338–51

103. Chhem RK, Wang S, Jaovisidha S, et al. Imaging of fungal, viral, and parasitic musculoskeletal and spinal diseases. Radiol Clin North Am. 2001;39:357–78.

104. Zainal AI, Wong SL, Pan KL, et al. Cryptococcal osteomyelitis of the femur: a case report and review of literature. Trop Biomed. 2011;28:444–9.

105. Pandey A, Bansal V, Asthana AK, et al. Maxillary osteomyelitis by mucormycosis: report of four cases. Int J Inf Dis. 2011;15:e66–e9.

106. Lindsley MD, Guarro J, Khairy RN, et al. Pseuallescheria fusoidea, a new cause of osteomyelitis. J Clin Microbiol. 2008;46:2141–3.

107. Cortez KJ, Roilides E, Quiroz-Telles F, et al. Infections caused by *Scedosporium* spp. Clin Microbiol Rev. 2008;21:157–97.

Suggested Reading

Davies SF. An overview of pulmonary fungal infections. Clin Chest Med. 1987;8:495–512.

DeLone DR, Goldstein RA, Petermann G, et al. Disseminated aspergillosis involving the brain: distribution and imaging characteristics. AJNR Am J Neuroradiol. 1999;20:1597–604.

Franquet T, Gimenez A, Hidalgo A. Imaging of opportunistic fungal infections in the immunocompromised patient. Eur J Radiol. 2004;51:130–8.

Gotway MB, Dawn SK, Caoili EM, Reddy GP, Araoz PA, Webb WR. The radiologic spectrum of pulmonary *Aspergillus* infections. J Comput Assist Tomogr. 2002;26:159–73.

Manning SC, Merkel M, Kriesel K, Vuitch F, Marple B. Computed tomography and magnetic resonance diagnosis of allergic fungal sinusitis. Laryngoscope. 1997;107:170–6.

Radin R. HIV infection: analysis in 259 consecutive patients with abnormal abdominal CT findings. Radiol. 1995;197:712–22.

Som PM. Imaging of paranasal sinus fungal disease. Otolaryngol Clin North Am. 1993;26:983–94.